


Non-destructive evaluation of critical current on a Bi-2212 first stage cable based on numerical analysis of the remnant field distributions

W Chen¹, X S Yang^{1,5} , Q B Hao², C S Li², J G Qin³, Y Wu³, J G Li³ and Y Zhao^{1,4,5}

¹ Key Laboratory of Magnetic Levitation Technologies and Maglev Trains (Ministry of Education), Superconductivity and New Energy R&D Center, Mail Stop 165#, Southwest Jiaotong University, Chengdu 610031, People's Republic of China

² Northwest Institute for Nonferrous Metal Research, Xi'an, 710016, People's Republic of China

³ Institute of Plasma Physics, CAS, Hefei 230031, People's Republic of China

⁴ College of Physics and Energy, Fujian Normal University, Fuzhou, Fujian 350117, People's Republic of China

E-mail: xsyang@swjtu.edu.cn and zhaoyong@fjnu.edu.cn

Received 27 February 2018, revised 1 October 2018

Accepted for publication 11 October 2018

Published 9 November 2018



Abstract

The high temperature superconducting material Bi-2212 is considered for use in the next generation of fusion reactors due to an excellent current carrying capacity in a high field. The critical current as well as its inhomogeneity are important factors in evaluating the performance of Bi-2212 wires, cables and conductors. Non-destructive evaluation by using a Hall sensor array is a more effective and faster method for testing the local critical current of a high temperature superconductor compared with a conventional contact-electrical method. In this paper, the coupling and decoupling numerical models of the perpendicular component of the residual magnetic field in Bi-2212 round wire were solved. Then, the perpendicular component of the remnant magnetic field was measured by a Hall sensor array, which was consistent with the results of the coupling model. Our results established the numerical model for a Bi-2212 first stage cable and found that the non-destructive method using four mutual vertical Hall sensor arrays is feasible for evaluation of cable critical current properties.

Keywords: Bi-2212, critical current, remanent magnetic field, Hall sensor array

(Some figures may appear in colour only in the online journal)

1. Introduction

A Bi-2212 multifilamentary composite structure which contains a Bi-2212 superconducting phase and a Ag alloy sheath can be commercially made into round wire with an isotropic cross section, which has excellent properties under low temperature, high magnetic field conditions [1–3]. The unique feature of Bi-2212 is that it is the only high temperature superconductor

(HTS) conductor that can provide a high critical current density in the macroscopic isotropy. For example, Bi-2212 round wire can be easily wound into a solenoid coil, and is compatible with conventional cabling technology. Bi-2212 has potential applications as a cable in conduit conductor for high-field superconducting magnets in future fusion reactors such as the China Fusion Engineering Test Reactor [4–6].

The critical current (I_c) is one of the most important factors for evaluating the performance of Bi-2212 wires, cables and conductors [7]. In addition, the Bi-2212 phase is

⁵ Authors to whom any correspondence should be addressed.

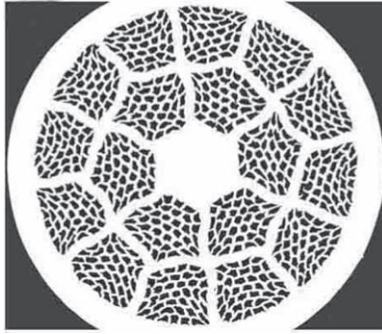


Figure 1. The cross-sectional image of the Bi-2212 round wire.

brittle and sensitive to strain, with poor mechanical properties [8–10]. The strain can easily lead to the production of local microcracks, causing inhomogeneity of the critical current. With this increase of inhomogeneity, heat spots may appear more frequently and the AC loss may increase [11, 12]. Therefore, it is necessary to evaluate and simulate the critical current distribution in practical applications.

The Hall sensor method is one of the most useful non-destructive methods for evaluation and simulation of the critical current distribution for high temperature superconductors [13–15] and MgB_2 [16]. With higher spatial resolution, more local I_c degradation could be detected by a Hall sensor array system compared to a normal four-probe method. The remnant or shielding field on the surface of HTS tape can be measured continuously by a Hall sensor and the local critical current will be evaluated [17–20]. Higashikawa *et al* used reel-to-reel scanning Hall-probe microscopy to evaluate the local critical current distribution for a multi-filamentary coated conductor [21]. In this work, we set up a numerical model for coupling and decoupling Bi-2212 round wire under a critical state and compared the numerical results of the residual magnetic field with the test results. It was found that the coupling model was more consistent with the actual measurement value. In addition, the coupling numerical model of Bi-2212 first stage cable was established. We proposed effective detection of the inhomogeneity of the critical current by using four mutual vertical arrays. These results proved that critical current of Bi-2212 cable could be non-destructively evaluated by using a Hall sensor array.

2. Numerical model and experimental measurement

2.1. Numerical model for Bi-2212 round wire

The Ag-alloy sheathed Bi-2212 round wire was manufactured using the powder-in-tube method [22]. The cross-sectional image of the sample is shown in figure 1. The geometrical parameters and the value of the critical current, I_c , of the wires are listed in table 1, where the value of I_c was measured by a transport four-probe method.

In figure 2, we set the Cartesian coordinate system in the center of the cross section of the wire and cable. The cross section of the wire and cable is the X–Z plane, and its length is along the Y direction. All the models below are built

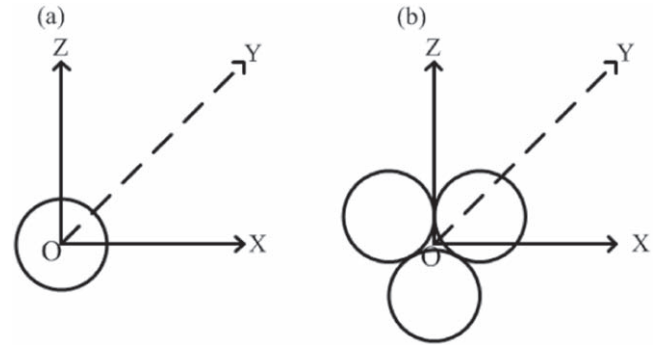


Figure 2. Computational model with a Cartesian coordinate system. (a) Round wire model. (b) Cable model.

Table 1. Parameters of the Bi-2212 round wires.

Item	Round wire
Material	Ag-alloy sheathed Bi-2212
Outer diameter	1 mm
Inner diameter	0.86 mm
Filament configuration	37×18
I_c , 0 T, 4.2 K	400 A
I_c , 12 T, 4.2 K	146 A
I_c , 0 T, 77 K	11 A

according to this coordinate system. In our numerical model of Bi-2212 round wire, the coupling model assumes that the superconducting core and the silver material between the cores are a whole, and the solution in the decoupling model assumes that the current density is only distributed in the superconducting core where shown in figure 3. $+J$ and $-J$ indicate the distribution of current density in the superconducting wire under the critical state [23], and the value of J was obtained by the four-probe method. The remnant magnetic field in the numerical model was calculated based on the assumption that the above mentioned transport current density J was equal to the magnetization current density.

2.2. Measuring method for the Bi-2212 round wire

The Hall sensor array system is shown in figure 4. The perpendicular component of the remnant field B_z around the Bi-2212 round wire was measured by a Hall sensor array after applying an external perpendicular magnetic field by an electromagnet in a liquid nitrogen bath within a cryostat. The electromagnet provided the magnetic field of 0.2 T in a 3 mm gap and the magnetic direction was perpendicular to the wire axis. The Hall sensor array (AREPOC multi-7U) contained seven Hall sensors. The effective area of each sensor was $50 \mu\text{m} \times 50 \mu\text{m}$, and the distance between each of the Hall sensors was 0.5 mm. A Hall array holder, made of machinable ceramic, was used as shown in figure 4. The surface of the holder was smooth enough to not damage the Bi-2212 round wire by sliding friction. The distance between the active area of the Hall array and the surface of the round wire was kept at a constant value of 0.56 mm, shown in figures 3(a) and (b)

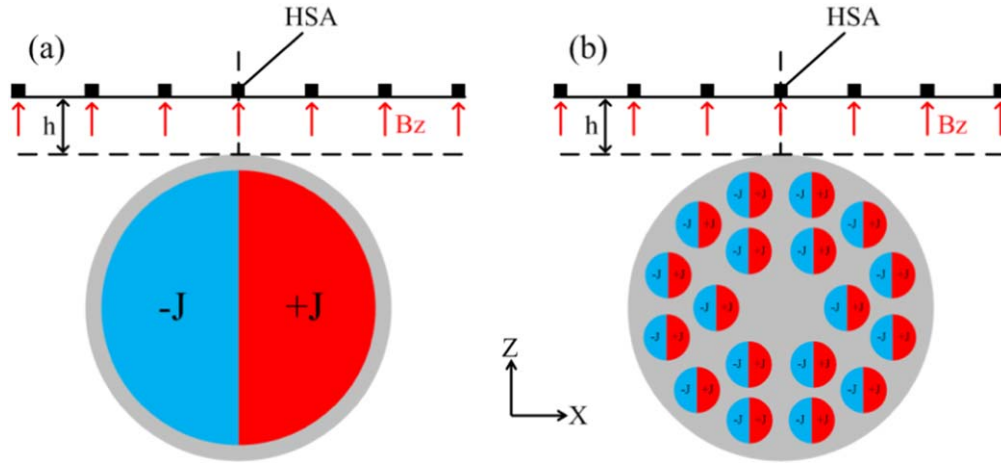


Figure 3. Schematic diagram of (a) the coupling numerical model and (b) the decoupling numerical model of Bi-2212 round wire.

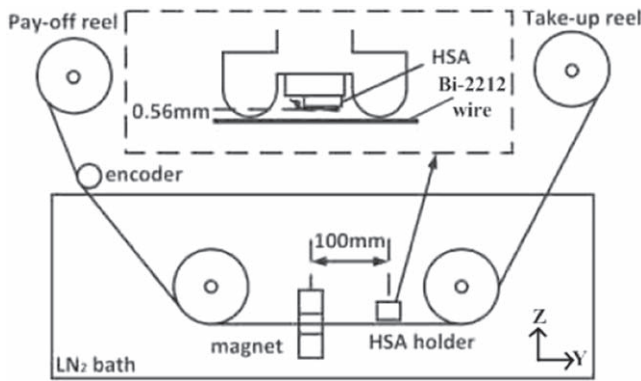


Figure 4. Diagram of the Hall sensor array (HSA) system.

($h = 0.56$ mm). The distance between the electromagnet and the Hall array holder was about 100 mm and the effect of the magnetic relaxation could be ignored. The measurement speed was 10 mm s^{-1} while the longitudinal spatial resolution was 0.4 mm.

2.3. Numerical model for the Bi-2212 cable

The Bi-2212 cable was made of three twisted Bi-2212 round wires, as shown in figure 5(a). The twist pitch of the Bi-2212 cable is 60 mm. Figure 5(b) shows the distance of four mutually perpendicular Hall arrays from the cable surface. The section along the length of the cable at different locations is shown in figure 5(c). Figure 5(d) describes the relationship between angles and different lengths of cables. According to the periodic structure of the cable, 0° – 120° means $1/3$ of the cable twist pitch length, which is 0–20 mm.

3. Results and discussion

3.1. Numerical solution and experimental measurement of remnant magnetic for the Bi-2212 round wire

Figure 6 is the z component of the remnant magnetic field in the Bi-2212 round wire with coupling and decoupling

models. The maximum value of the remnant magnetic field in the coupling model is 4.7 mT, which is concentrated on the vertical plane in the round wire. The maximum value of the remnant magnetic field in the decoupling model is 0.82 mT, which is concentrated on the middle vertical surface of the superconducting core. The Hall probe array is used to measure the vertical component of the residual magnetic field of the Bi-2212 round wire, and the surface distance array of the round wire is 0.56 mm. In the numerical model, in order to compare with the experimental results, we also extract the vertical component of the residual magnetic field at the 0.56 mm position at the surface of the Bi-2212 round wire. In figure 7, Hall sensor array data represent test values. The measured B_z values along the length of the round wire by the Hall sensor array method are combined into one plot for comparison. The positions along the radial of the wire are marked with \times . In the continuous measuring process, as there is little disturbance, the round wire has small offsets in the X direction. A laser displacement sensor was used to record the offsets between the wire and the Hall sensor. In the finite element solution, we can see that the maximum values of the vertical components of the residual magnetic field in the coupled model and the decoupled model are 0.1 mT and 0.01 mT, respectively. The numerical results of the coupled model are in good agreement with the experimental values. Similar results have been reported in [23]. Therefore, in the numerical model of the Bi-2212 cable, the coupling model will be used.

3.2. Bi-2212 cable remnant magnetic numerical solution

It is difficult to test the inhomogeneity of the critical current in the length direction of the Bi-2212 cable with a single array. In the direction of the cable length, the distribution of the vertical component of the radial residual magnetic field along the cable is changed by a single array. In this work, we propose to use four mutual vertical Hall sensor arrays to detect the residual magnetic field of the Bi-2212 first cable. Figures 8(a) and (b) are the z component and x component of the remnant magnetic field in the Bi-2212 cable with the coupling model at 4.2 K, respectively. The maximum value of the z component of the residual magnetic field is 180 mT, and

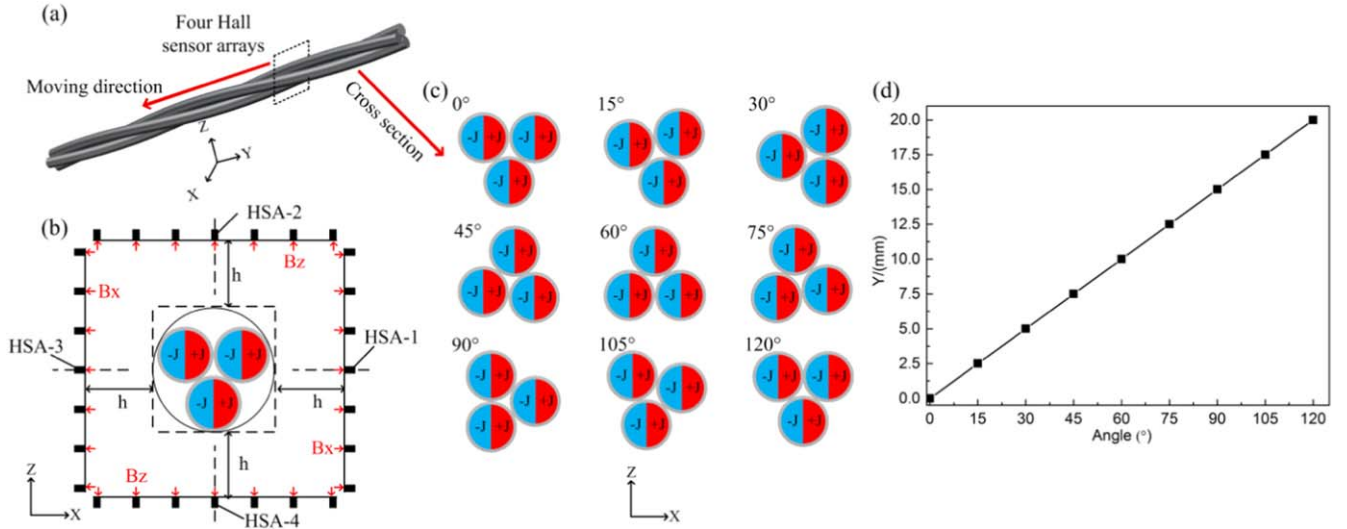


Figure 5. (a) Schematic diagram of the Bi-2212 cable. (b) The distance of four mutually perpendicular Hall arrays from the cable surface. (c) Coupling numerical model of the Bi-2212 cable with different cross sections. (d) The relationship between the different sections and angles of the Bi-2212 cable along the length direction (Y direction).

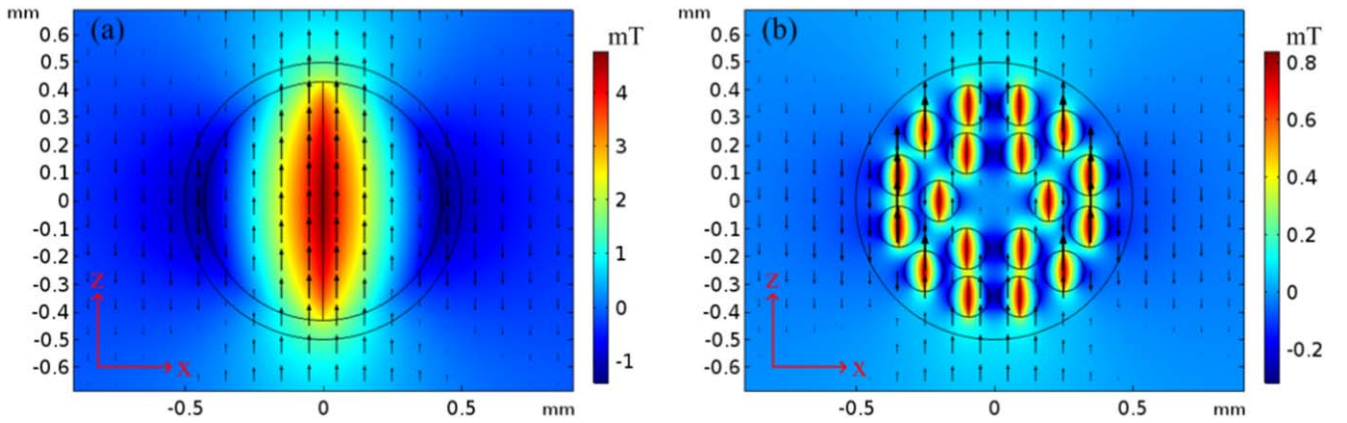


Figure 6. (a) The z component of the remnant magnetic field in the Bi-2212 round wire with the coupling model at 77 K. (b) The z component of the remnant magnetic field in the Bi-2212 round wire with the decoupling model at 77 K. The black arrows indicate the magnetic flux density vector in the z direction.

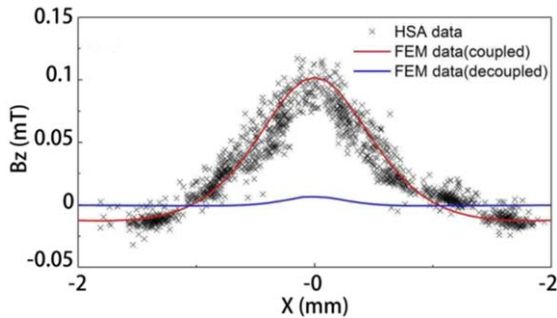


Figure 7. The numerical solution and experimental values of the remnant magnetic field of the Bi-2212 round wire along the radial distribution at 77 K.

the maximum value of the x component of the remnant magnetic field is 80 mT. The upper and lower arrays in figure 5(b) detect the z component of the residual magnetic field of the Bi-2212 cable. The left and right arrays in

figure 5(b) detect the x component of the remnant magnetic field. Figure 9 shows the residual magnetic field distribution at different positions along the length of the Bi-2212 cable detected by four mutually perpendicular Hall sensor arrays. The distance between the Hall array and the cable surface is $h = 0.56$ mm. 0° , 15° , and 30° represent 0 mm, 2.5 mm, and 5 mm along the length of the cable, respectively. The distribution of the residual magnetic field detected by each Hall sensor array varies with the length of the cable. Therefore, a single Hall sensor array cannot calibrate its critical current inhomogeneity. Figure 10 shows the sum of the remaining magnetic fields of the Bi-2212 cable detected by four Hall arrays. B_{sum} is calculated by equation (1):

$$B_{\text{sum}} = B_{x(\text{HSA}-1)} + B_{z(\text{HSA}-2)} + B_{x(\text{HSA}-3)} + B_{z(\text{HSA}-4)}. \quad (1)$$

The transverse coordinates of figure 10 are expressed in different positions along the cable length. In this work, the length is $1/3$ of the twist pitch length. B_{sum} keeps almost the

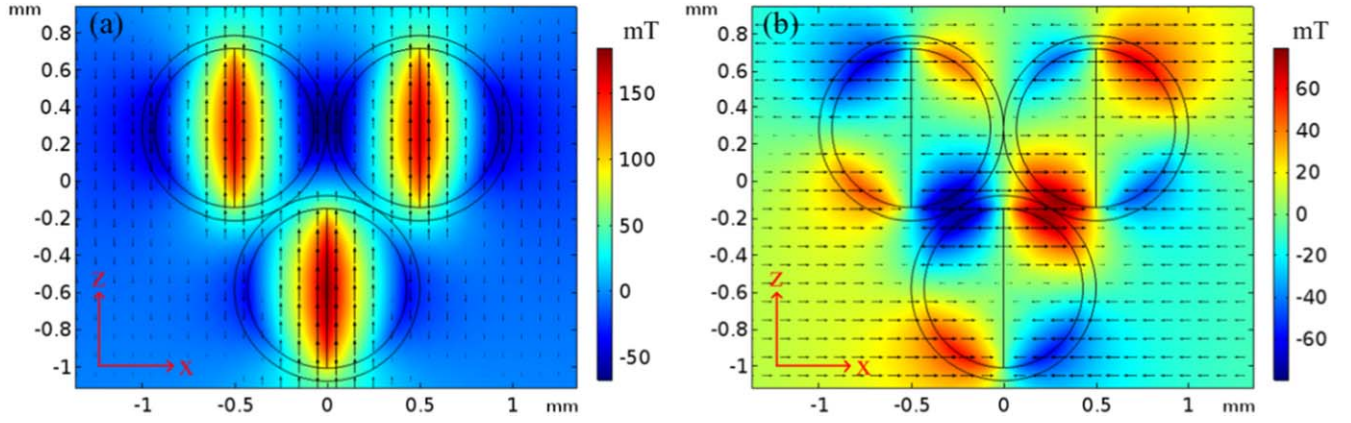


Figure 8. (a) The z component of the remnant magnetic field of the Bi-2212 cable at 4.2 K. (b) The x component of the remnant magnetic field of the Bi-2212 cable at 4.2 K. The black arrows indicate the magnetic flux density vector in the z or x direction.

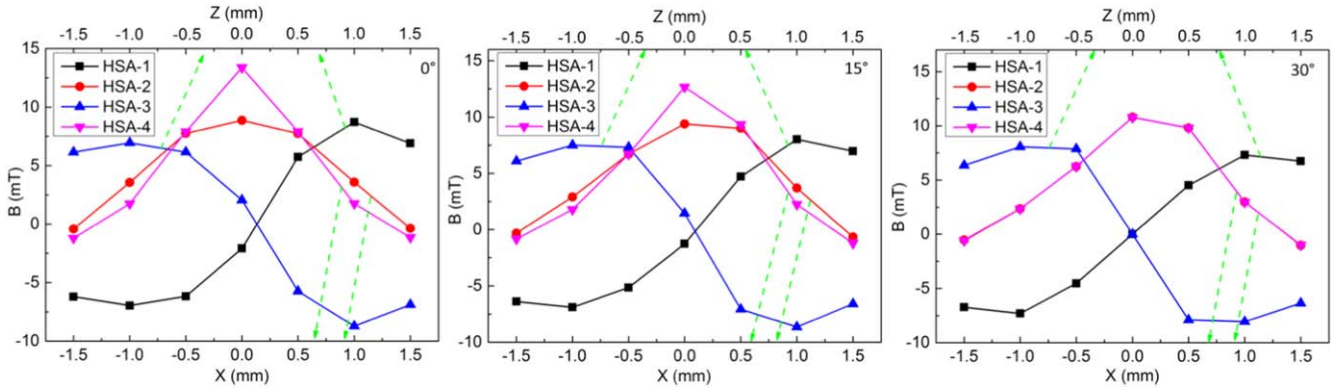


Figure 9. Remnant magnetic fields of the first Bi-2212 cable at 4.2 K detected by four Hall sensor arrays. The green dotted lines indicate the coordinates of the probe in different Hall arrays.

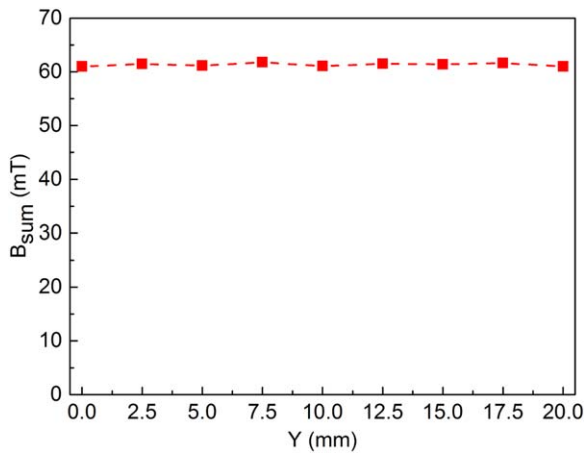


Figure 10. Sum of the remaining magnetic fields of the first Bi-2212 cable at 4.2 K detected by four Hall arrays.

same value with the change of position. Therefore, the inhomogeneity of the critical current (relative I_c) of the Bi-2212 cable is obtained by detecting the B_{sum} of the remaining magnetic fields using four Hall sensor arrays.

Accordingly, the actual I_c along the length of the cable will be obtained after calibration using the result of the four-probe method.

4. Conclusion

The coupling and decoupling numerical models for Bi-2212 round wire are used to solve the vertical component of the residual magnetic field along the radial distribution under the critical state. The comparison of the numerical and experimental results shows that the coupling model is more consistent with the actual measured values. On this basis, we set up a Bi-2212 cable coupling numerical model at 4.2 K and propose the use of four mutually perpendicular arrays to detect the residual magnetic field of the cable. The results show that the four arrays can detect the inhomogeneity of the critical current of the first cable. This method is also useful for detecting critical current non-uniformities in multi-filament superconducting cables such as NbTi, Nb₃Sn, and MgB₂ using a non-destructive method. Next, we will establish a more practical magnetic field affecting the critical current

model with a multi-stage stranded strand, and use four Hall sensor arrays to test the inhomogeneity of the critical current at 4.2 K. Finally, a non-destructive evaluation of the critical current for Bi-2212 second, third and full-scaled conductor will soon be discussed.

Acknowledgment

This work was supported by the National Magnetic Confinement Fusion Science Program (grant no. 2017YFE0301402).

ORCID iDs

X S Yang  <https://orcid.org/0000-0002-8686-9860>

References

- [1] Shen T, Li P, Jiang J, Cooley L, Tompkins J, McRae D and Walsh R 2015 *Supercond. Sci. Technol.* **28** 065002
- [2] Mao Z, Jin H, Qin J, Liu F, Dai C, Hao Q and Li C 2017 *IEEE Trans. Appl. Supercond.* **27** 6400405
- [3] Liu L, Chen W, Shi J, Li C, Hao Q, Pan M, Yang X, Zhang Y and Zhao Y 2017 *Fusion Eng. Des.* **124** 86–9
- [4] Brown M, Bosque E, McRae D, Walsh R P, Jiang J, Hellstrom E E, Kim Y, Trociewitz U, Otto A and Larbalestier D C 2017 *IOP Conf. Ser.: Mater. Sci. Eng.* **279** 012022
- [5] Liu F, Liu H, Qin J, Li J, Wu Y, Shi Y, Ci L, Lei L and Jin H 2017 *Fusion Eng. Des.* **122** 228–31
- [6] Qin J *et al* 2018 *Supercond. Sci. Technol.* **31** 015010
- [7] Rey J M, Allais A, Duchateau J L, Fazilleau P, Gheller J M, Bouter R L, Louchard O, Quettier L and Tordera D 2009 *IEEE Trans. Appl. Supercond.* **19** 3088–93
- [8] Qin J, Dai C, Wang Q, Liu P, Liu B, Li C, Hao Q and Zhou C 2016 *IEEE Trans. Appl. Supercond.* **26** 8402107
- [9] Bjoerstad R, Scheuerlein C, Rikel M O, Ballarino A, Bottura L, Jiang J, Matras M, Sugano M, Hudspeth J and Michiel M D 2015 *Supercond. Sci. Technol.* **28** 062002
- [10] Godeke A, Hartman M H C, Mentink M G T, Jiang J, Matras M, Hellstrom E E and Larbalestier D C 2015 *Supercond. Sci. Technol.* **28** 032001
- [11] Wang Y, Dai S, Zhao X, Xiao L, Lin L and Dong H 2006 *Supercond. Sci. Technol.* **19** 1278–81
- [12] Zhu Y, Chen W, Zhang H Y, Liu L Y, Pan X F, Yang X S and Zhao Y 2018 *Supercond. Sci. Technol.* **31** 035007
- [13] Kim H *et al* 2010 *IEEE Trans. Appl. Supercond.* **20** 1537–40
- [14] Higashikawa K *et al* 2014 *IEEE Trans. Appl. Supercond.* **24** 6600704
- [15] Lao M, Hecher J, Sieger M, Pahlke P, Bauer M, Hühne R and Eisterer M 2017 *Supercond. Sci. Technol.* **30** 024004
- [16] Higashikawa K, Tatara H, Inoue M, Ye S, Matsumoto A, Kumakura H and Kiss T 2016 *IEEE Trans. Appl. Supercond.* **26** 6200804
- [17] Roth B J, Sepulveda N G and Wikswo J P Jr 1989 *J. Appl. Phys.* **65** 361–72
- [18] Ušák P 2003 *Physica. C* **384** 93–101
- [19] Xing W, Heinrich B, Zhou H, Fife A A and Cragg A R 1994 *J. Appl. Phys.* **76** 4244–55
- [20] Herrmann J, Savvides N, Müller K H, Zhao R, McCaughey G, Darmann F and Apperley M 1998 *Physica C* **305** 114–24
- [21] Higashikawa K, Uetsuhara D, Inoue M, Fujita S, Iijima Y and Kiss T 2017 *IEEE Trans. Appl. Supercond.* **27** 6603004
- [22] Zhang S, Li C, Hao Q, Feng J and Zhang P 2017 *Rare Metal Mat. Eng.* **46** 585–90
- [23] Baba S, Inada R, Makihara T, Nakamura Y, Oota A, Sakamoto S, Li C S and Zhang P X 2010 *J. Phys.: Conf. Ser.* **234** 022004